

2023

Heat Transfer of Non-Newtonian Drag Reducing Flow in Porous Media

Mohamed Alaa Zahran

Follow this and additional works at: <https://digitalcommons.aaru.edu.jo/erjeng>

Recommended Citation

Alaa Zahran, Mohamed (2023) "Heat Transfer of Non-Newtonian Drag Reducing Flow in Porous Media," *Journal of Engineering Research*: Vol. 7: Iss. 2, Article 13.

Available at: <https://digitalcommons.aaru.edu.jo/erjeng/vol7/iss2/13>

This Article is brought to you for free and open access by Arab Journals Platform. It has been accepted for inclusion in Journal of Engineering Research by an authorized editor. The journal is hosted on [Digital Commons](#), an Elsevier platform. For more information, please contact rakan@aar.edu.jo, marah@aar.edu.jo, u.murad@aar.edu.jo.

Heat Transfer of Non-Newtonian Drag Reducing Flow in Porous Media

M.A. Zahran^{1*}, M.S. El-Kady², L.H. Rabie², Waleed M. ElAwady²

¹Mechanical Power Engineering Department, Faculty of Engineering, Mansoura University, Egypt – email: mohamedzahran5426@gmail.com

²Mechanical Power Engineering Department, Faculty of Engineering, Mansoura University, Egypt

Abstract- Forced convection heat transfer for non-Newtonian drag reduction (polyethylene oxide) with heat flux is experimentally studied in a pipe filled with plastic spheres porous media. Along the pipeline, installing pumping stations is expensive; reducing the drag inside the pipe is better. The effect of PEO concentration on the heat transfer properties in the pipe is studied. The experiments are used to demonstrate the effect of changing Reynolds number and PEO concentrations on Nusselt number of the water and polymer solutions for different diameter ratios (d/D) and different concentrations. In the experiments, the test section is a circular pipe filled with plastic spheres of different diameters (3.3, 5.5, and 6.8 mm). The test section is covered by an electric heater made of nickel-chromium with a mica sheet to warm it with uniform heat flux (UHF). Thermocouples (k-type) are used to measure the temperatures of water and different concentrations of polyethylene oxide solution (50, 100, 150, and 200 ppm). The results show that Nusselt number increase with increasing Reynolds number in water and polymer solutions (PEO). The local Nusselt number and Nusselt number increase with increasing diameter ratios (d/D) of porous media for water and polymer solutions (PEO). The thermal entrance length is independent on PEO concentration and diameter ratios but depends only on Reynolds number. Correlations of the thermal entrance length as a function of Reynolds number and of Nusselt number as a function of Reynolds number and diameter ratio (d/D) are obtained.

Keywords- heat transfer, drag reducing, non-Newtonian, porous media, polyethylene oxide.

1- INTRODUCTION

The non-Newtonian fluid behavior in porous media differs from Newtonian fluids in porous medium. In recent years, the study of heat transfer in non-Newtonian fluids in porous media has drawn a lot of attention because it has numerous important engineering and scientific applications, including food processing, nuclear waste storage, the transportation of chemicals, and the discovery of the flow of oil in petroleum reservoirs. Many industrial processes, including those in the chemical and oil sectors, use non-Newtonian fluid flows through porous media that have features that reduce drag. [1-3]

Drag is the reduction in flow rate brought on by pressure head losses inside a pipe. Along the pipeline, more pumping stations are being installed to supply energy and maintain the required flow rate in order to combat the declining flow rate [4]. As a result, installing pumping stations is expensive and impractical from an economic standpoint. By reducing the drag inside the pipe, this problem can also be solved. This method is known as drag reduction (DR) [5]. Rabie and Mustafa [6] investigate the heat transfer in pulsating laminar flow experimentally for drag reduction in diluted solutions. Drag polymer solutions reducing (Polyacrylamide) flow

through the annulus of the tubular heat exchanger, while hot water from a heating source flows steadily through the inner pipe. Different polymer concentrations are considered at 10, 25, and 100 ppm, showing that for steady laminar flow, there is hardly any difference between Nusselt number for drag reducing flow and those water flows.

Raei et al [7] experimental research was done to determine how adding a polymer drag-reducing agent affected, heat transfer, water flow, and pressure drop. A double pipe heat exchanger was used with aqueous solutions of polyacrylamide (PAM) in various concentrations (up to 100 ppm) with fully developed turbulent flow. In contrast to earlier studies, there was little drag reduction from using PAM. Even at low concentrations, the addition of PAM significantly reduced heat transfer.

Lv and Zhang [8] investigated the heat transfer and drag reduction properties of water flow through pipes with super hydrophobic surfaces. Super hydrophobic tubes had lower heat transfer coefficients than smooth tubes. Sears and Yang [9] the heat transfer coefficients for a surfactant-drag-reducing solution in the entrance region of a uniformly heated horizontal cylindrical tube with Reynolds numbers ranging from 25,000 to 140,000 and temperatures ranging from 30 to 70 °C are measured. It was discovered that the heat transfer coefficients decreased along with the drag reduction.

Varnaseri and Peyghambarzadeh [10] examined the efficiency of water flow and heat transfer inside horizontal, smooth circular pipes at various heat fluxes to determine the impact of polyacrylamide (PAM) addition as a drag-reducing agent. The heat transfer reduction (HTR) properties of solutions containing (DRAs) are one of the drawbacks of using these materials. According to the results, adding a drag reducing polymer reduces heat transfer.

Chamkha [11] various studies have looked at the convection heat transfer from wedges inserted in porous media and on vertical surfaces. This is because these flows have various geophysical applications, and the reduced local Nusselt and Sherwood numbers were found to increase the buoyancy ratio.

Rashad et al. [12] investigated non-Newtonian fluid heat transfer from surfaces through porous media using laminar boundary layer flow and discovered that in the pure free convection regime, the power-law fluid index increased as Sherwood and the local Nusselt numbers reduced. Tian et al. [13] demonstrate heat transfer fluid flow and power law properties. Experimental research was done with spheres packed into beds. The working fluids are selected to be partially dissolved solutions (HPAM) at various temperatures and

concentrations. The results would be helpful for the best-suited design of packed beds. The heat transfer coefficient gradually decreased as Reynolds numbers and HPAM concentrations increased.

Kairi and Murthy [14] study the impact of heat and mass transfer from a vertical cone in a non-Darcy porous medium filled with a non-Newtonian fluid with viscous dissipation. For both assisting and obstructing buoyancy cases with all varieties of power law fluids, it was discovered that as the viscosity Sherwood number rises, Nusselt number decreased. Peixinho and Lebouche [15] investigate experimentally the non-Newtonian fluid flow for forced convection heat transfer in a pipe. A heat flux condition for wall boundary heating is mandated. Aqueous solutions of carbopol (polyacrylic acid), a non-Newtonian fluid, are employed. It was located where similar critical Reynolds numbers apply to heat.

Rao [16] studied the pressure drop and heat transfer for the flow of carbopol 934® and carbopol ez1® aqueous solutions through a vertical tube filled with porous medium. The heated stainless steel test section measures 200 diameters long and has an interior diameter of 2.25 cm. Direct electric current through the tube wall was used to impose a uniform heat flux thermal boundary condition, which demonstrated that heat transfer to the power law increases with increasing Reynolds number.

Zhang et al. [17] studied how frictional pressure drop and heat transfer in a two-phase flow of water and air were affected by polyacrylamide, a drag-reducing agent. They reported a 70.3% reduction in heat transfer and a 54.7% reduction in pressure drop. Shenoy [18] presented a number of intriguing applications of fluids with yield stress and non-Newtonian power laws on convective heat transfer in fluid-saturated porous media, with a focus on oil reservoirs and engineering geothermal.

EI-Kady [19] studies forced convection heat flow through a saturated porous media-filled circular pipe that is subjected to constant heat flux. Ai-Hamad and Duwairi [20] presented a non-Newtonian power-law fluid's mixed convection heat transfer in a cylinder embedded in a porous medium. It was discovered that the velocity profiles within the boundary layer and the local Nusselt number decreased as the power law index increased. But the temperature profiles increased. The decrease of the local Nusselt number has also been discovered.

Atwan et al. [21] studied the experimental flow and heat transfer properties in horizontal annuli that included porous media. The average Nusselt number for air rises as the particle conductivity of the working fluid increases. Also, as the radius ratio rises, the average Nusselt number rises. EIKady et al. [22] investigated experimentally in an inclined annulus of porous media with a warmed inner cylinder and a constant temperature cooled outer cylinder, laminar natural convection of air occurs. They show that with increasing porosity, the total heat transfer coefficient and the average Nusselt number increase.

Elkady [23] stated that an increase in Reynolds numbers is caused by a decline in the highest temperature of both heat

sources and a rise in the local average Nusselt number, according to an experimental investigation of laminar mixed convection in a partially filled porous medium. Mahgoub [24] non-Darcian conducted an experimental study of forced convection heat transfer over a flat horizontal plate in a porous media of spherical particles. The effects of particle diameter and particle materials with various thermal conductivities were investigated using air as the working fluid. It was discovered that larger particle sizes and higher particle thermal conductivity led to higher heat transfer coefficients.

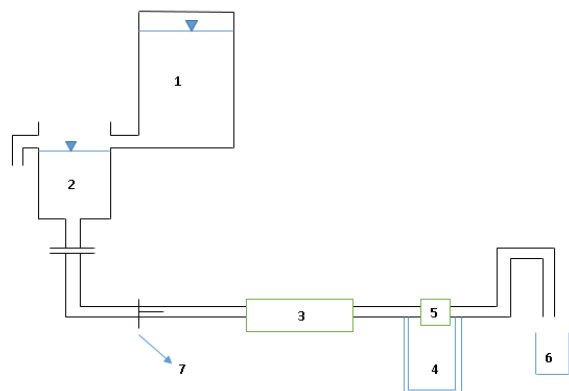
Zhang et al. [25] investigated numerically the two-dimensional heat transfer and steady flow through a porous particle with a constant temperature placed in a cold fluid. It demonstrates the effects of Darcy and Reynolds number on the flow and heat transfer characteristics by using the lattice Boltzmann method. It is found that the averaged Nusselt number and heat-transfer enhancement ratio almost linearly increased with increasing Reynolds number, and when Reynolds number increased, the local Nusselt number increased.

From the literature review, it is found that a little works for the drag reducing fluid in porous media, and there are still many unanswered questions. New experimental data on the properties of heat transfer for polyethylene oxide solutions at different concentrations (50, 100, 150, and 200 ppm) is presented. The PEO concentrations pass through a porous medium packed with different diameter plastic spheres (3.3, 5.5, and 6.8 mm) in a cylinder cross-section pipe. It presents the study's results, which offer insight into the heat transfer process in drag reducing fluid flowing through particle-filled porous media.

II- EXPERIMENTAL SETUP

A. Experimental setup

The experimental system, shown schematically in Figure 1, is an open-loop pipeline system that includes a plastic (PVC) tank (1) with a 500-liter capacity that serves as an overhead tank. The little tank with a constant head overflow (2) that is supplied by this tank is situated 6.0 m above the test section (3).

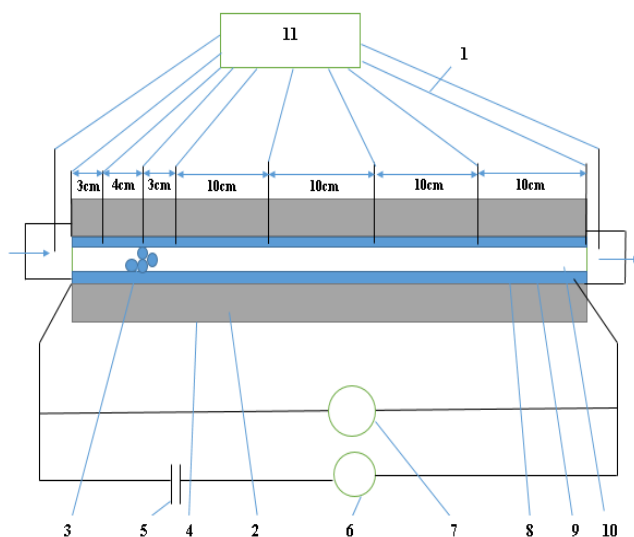


1) Overhead Tank 2) Constant head tank 3) Test section
4) U-tube Manometer 5) Orifice Meter 6) collector 7) Valve

Fig. 1. Schematic diagram of experimental apparatus.

Gravity causes the fluid to drain from the overflow tank. The test section is constructed from a copper tube that is 50cm long and 2.54 cm inside diameter. The pipe is uniformly filled with plastic spheres of the same size to form a packed bed that serves as a solid, porous matrix that acts as a conduit for fluid. Spheres with different diameters are used throughout this work. In the gravitational open flow system, the porous section is kept horizontal. To test the effect of particle spheres diameter, a different diameters are used (3.3, 5.5, and 6.8) mm, which gives diameter ratios $d/D = 0.123, 0.22,$ and $0.272,$ respectively. With porosity of spheres in the test section of 0.37, 0.5, and 0.56, respectively. A calibrated orifice-meter (5) is used as a flowmeter to measure the high flow rates, which are used to determine the average velocity and Reynolds number of the flow. Outlet flow is collected into a 2 litre flask (6) for low flow rates. The time of filling is measured, and the outlet flow rate is determined. The wire mesh at the two ends of the pipe holds the spheres in place. The tested tube was heated electrically by an electrical heater. Experimental work was done by carrying out a series of measurements of temperatures and flow rates using either water flow or PEO concentrations of 50, 100, 150, and 200 ppm.

Figure 2 displays a schematic diagram of the test section. The test section is made of a copper tube (10) [2.54 cm inside diameter and 50 cm long]. The tested tube is heated electrically by an electrical heater. A nickel-chromium wire (9) is used as the electrical heater. The tested tube is covered by a mica sheet (8), which acts as an electrical insulating sheet, which then is covered by layers of fiberglass (2) of a thickness of about 3 cm. Finally, the test section is covered by aluminum foil (4) to reduce the heat loss from the electrical heater.



- (1) Thermocouples (2) Fiberglass (3) spherical particles (4) Aluminum foil
 (5) Auto – transformer (6) Ammeter (7) Voltammeter (8) mica sheet
 (9) Nickel-chromium electric heater wire (10) copper tested tube
 (11) Temperature Recorder

Fig. 2. Schematic diagram of the test section.

Thermocouples (K-type) (1) are used to measure the temperature of the test section. The surface temperature of the heated tube is measured by 8 thermocouples along the tube at a distance of 0, 3, 7, 10, 20, 30, 40, and 50 cm from the entrance of the heated tube. Another two thermocouples are used to measure the water and PEO solution flow temperatures at both the inlet and exit sections of the heated tube. The thermocouples are collected to a temperature recorder (11) to measure the temperature at each thermocouple. An autotransformer (5) is used to control the heat input to the test section, as well as a voltmeter (7) is used to measure the voltage acting on the heater and an ammeter (6) to measure the current. Readings of the measured volt and current are used to calculate the amount of electric power used by the heater, which has a heating power of 147.4 W.

B. Polymer characterization and fluid preparation

Polyethylene oxide (PEO), which has a molecular weight (MW) of 5×10^6 g/mole, was the polymer used in this study. The product was bought from Sigma-Aldrich in the US. The following relation can be used to prepare the polymer concentration by Abdul Latif [26]:

$$C(ppm) = \frac{m_s(mg)}{V_w(litre)} \quad (1)$$

where C is the needed PEO concentration, which is calculated in ppm, and m_s is the solute's mass, which is measured in mg. V_w is the solvent's volume, measured in litres, while the density of water means that there are 1000 grams of mass per 1 liter of volume.

The known volume of water was then covered with polyethylene oxide powder and left to sit for 24 hours in a beaker. With the aid of a magnetic bead, the solution was stirred. In order to prevent polymer degradation while preparing the sample, the mixture was stirred slowly and quietly in one direction until it became homogeneous. Before use, the mixture was allowed to fully melt and become homogeneous for at least 12 hours. These solutions were then diluted in an overhead tank to achieve the desired test solution concentration. The volume of mixture drawn from the stock sample is determined using the relation shown below [26]:

$$V_{st} = \frac{C_n V_n}{C_{st}} \quad (2)$$

where C_{st} is the stock concentration that was previously known, V_{st} is the volume of the stock sample, and C_n is the needed concentration.

III- THEORITICAL BACKGROUND

The experiments are used to illustrate how a variation in heat transfer coefficient and Nusselt number for water and polymer solutions can be caused by changing Reynolds number and PEO concentration.

The total heat transfer (input power) Q_{heater} by Atwan et al. [21] at steady state is the sum of Q_{net} due to convection heat transfer, convection and conduction heat losses.

$$Q_{\text{net}} = m \cdot C_p (T_{\text{bo}} - T_{\text{bi}}) \quad (3)$$

where C_p specific heat, m mass flow rate, T_{bo} and T_{bi} are the fluid temperatures of water at the outlet and inlet test section.

The local heat transfer coefficient h_x would be obtained as follows [21]:

$$h_x = q_{\text{net}} / (T_{w,x} - T_{b,x}) \quad (4)$$

where $q_{\text{net}} = Q_{\text{net}} / (\pi DL)$.

$T_{w,x}$ is the local temperature at any pipe surface location.

$T_{b,x}$ is the local fluid temperature at a streamwise tube location.

D , L are the tested pipe diameter and length.

X is the local position in the flow direction.

Energy balance is used to determine $T_{b,x}$. The form of the energy equation used for this purpose is given in eqn. (4):

$$T_{b,x} = T_{b,i} + q_{\text{net}} (\pi D \Delta x / m C_p) \quad (5)$$

where Δx is the stream distance for the streamwise station of interest from the heater start, the average heat transfer coefficient h is defined as follows [21]:

$$h = q_{\text{net}} \cdot (1/L) \int_L \frac{dx}{(T_{w,x} - T_{b,x})} \quad (6)$$

The local Nusselt number h_x along the surface of the tested tube may be expressed in terms of the measured surface net heat flux and the surface temperature with respect to the thermal conductivity of the water, as follows [21]:

$$Nu_x = h_x D / k_f = q_{\text{net}} \cdot D / k_f (T_{w,x} - T_{b,x}) \quad (7)$$

where k_f is the fluid's thermal conductivity.

The tube length averaged Nusselt number was defined as [21]:

$$Nu = hD / k_f = D / (k_f L) \cdot \int_L h_x \cdot dx \quad (8)$$

The other dimensionless parameter that was used in the formulation of the results, Reynolds number Re is defined according to the following [27]:

$$Re = \rho V D / \mu (1 - \varepsilon) \quad (9)$$

where ρ and μ are water density and dynamic viscosity, while ε is porosity.

IV- UNCERTAINTY ANALYSIS

Eqn. (7) is used to determine the uncertainties in Nusselt number in order to calculate the uncertainty of the experiments. The uncertainty value (E) for any calculated or measured parameter (Z), such as Nusselt number, is computed

as follows:

$$Z = f(x_1, x_2, x_3, \dots, x_n) \quad (10)$$

The uncertainty in the resultant parameter E_z is expressed as follows:

$$E_z = \sqrt{\left(\frac{\partial Z}{\partial x_1} E_{x1}\right)^2 + \left(\frac{\partial Z}{\partial x_2} E_{x2}\right)^2 + \dots + \left(\frac{\partial Z}{\partial x_n} E_{xn}\right)^2} \quad (11)$$

where E_{x1} , E_{x2} and E_{xn} are the uncertainties in the independent variables x_1 , x_2 , and x_n , respectively.

$$RE = \frac{E_z}{z} \times 100 \quad (12)$$

where RE is a relative errors (percentage errors).

The uncertainty of various measured variables is listed in Table 1. The maximum uncertainty value of Nusselt number as a calculated parameter is 5.41% using the data from Table 1 and Eqn. (11).

Table 1. Uncertainty of measured variables

Measured variable	Uncertainty
Temperature	$\pm 0.2^\circ\text{C}$
Diameter of particle	$\pm 0.1\text{mm}$
Diameter of main pipe	$\pm 0.1\text{mm}$
Test section length	$\pm 1\text{mm}$
Number of spheres	± 10
Voltage	$\pm 0.1\text{Volt}$
Current	$\pm 0.1\text{Ampere}$

V- RESULTS AND DISCUSSION

The purpose of the experimental measurement is to analyse the heat transfer characteristics for various PEO concentrations in a pipe filled with different diameter spheres by heating the tested tube electrically with an electric heater.

A. Thermal entrance length

The representative temperature distribution for the tube filled with plastic sphere particles at $d/D = 0.22$ at Reynolds Number values of 157.3, 861.8, 1167.1, 1600.6, 2334.2, and 3734.8 is shown in Figure 3 for water flow. The departure of the wall temperature from straight line behavior at the upstream end of the test tube is primarily due to the absence of front side heating at the end. The region of fully developed heat transfer is indicated by the range over which the slope of the wall temperature is equal to the calculated fluid temperature slope.

Figure 3 shows that when the heat flux is constant, the temperature difference between the wall and flow is constant for a constant Reynolds number, but when Reynolds number varies, by increasing Reynolds number, the temperature difference decreases for a constant heat flux.

Figures 4 and 5 illustrate the relationship between thermal entrance length and PEO concentration. Figure 4 shows that if Reynolds number is constant for all concentrations, the thermal entrance length is independent on the concentration.

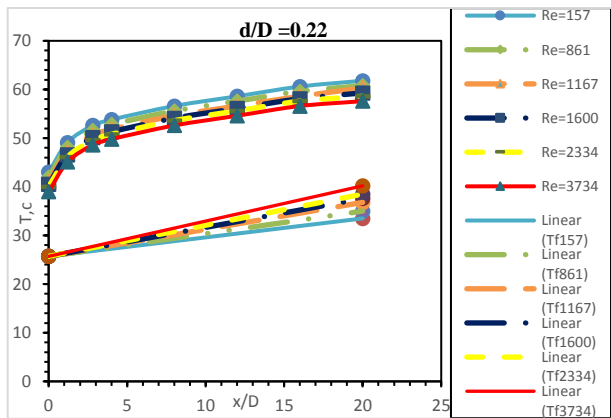


Fig. 3. Temperature distribution for a tube filled with a plastic sphere of $d/D = 0.22$ at different values of Reynolds number.

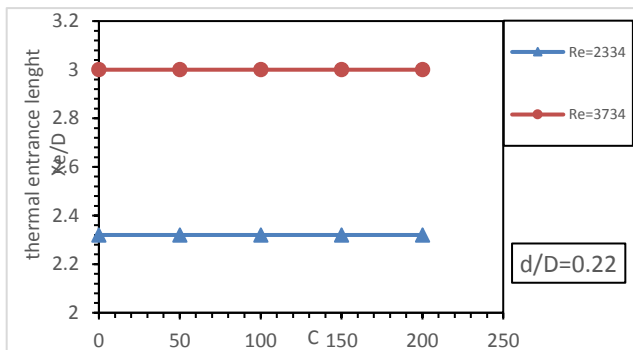


Fig. 4. The variation of the thermal entrance length at concentration with various values of Reynolds number.

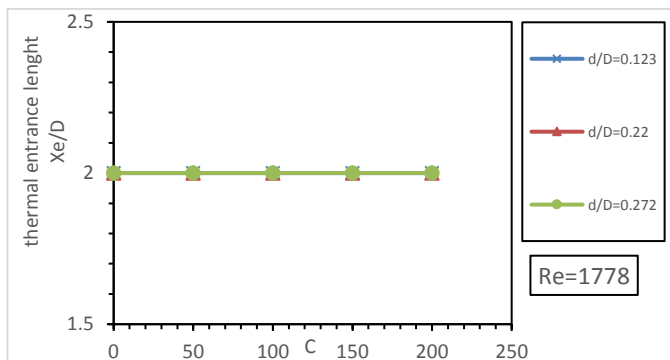


Fig. 5. The variation of the thermal entrance length with concentration for various values of diameter ratios (d/D).

In the same figure, two values for Reynolds number are used: 2334 and 3734 at all concentrations, and it is shown from the figure that the thermal entrance length does not depend on changing the concentration but only on changing Reynolds number.

Figure 5 shows the relationship between the thermal entrance length and PEO concentration for different diameter ratios $d/D = 0.123, 0.22,$ and 0.272 . When Reynolds number is constant at 1778 for the three diameter ratios, it is found that the thermal entrance length is not affected by the change in the diameter ratios, and therefore the three lines as shown in the figure are identical to each other. Because the thermal entrance

length depends only on the velocity at the beginning of the fluid entry to the pipe before it becomes fully developed and thus depends only on Reynolds number.

Figure 6 presents the thermal entrance length variation with the variation of Reynolds number for water and PEO concentration flows at concentrations of (50, 100, 150, and 200 ppm). The tube is filled with plastic sphere particles of different diameters $d/D = 0.123, 0.22,$ and 0.272 . The thermal entrance length depends only on Reynolds number, and a correlation can be obtained from the values of figure 6 as follows:

$$X_e/D = 0.0284Re^{0.5663} \quad (13)$$

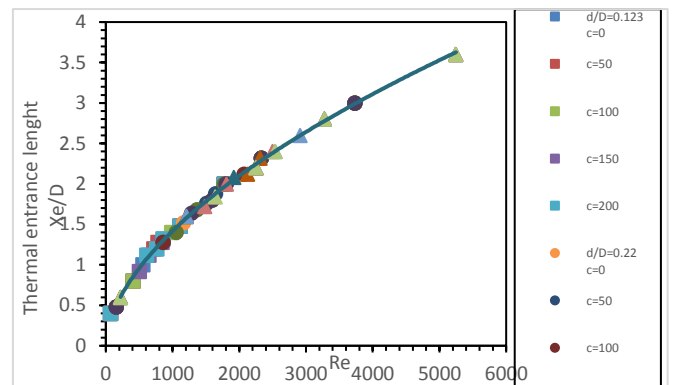
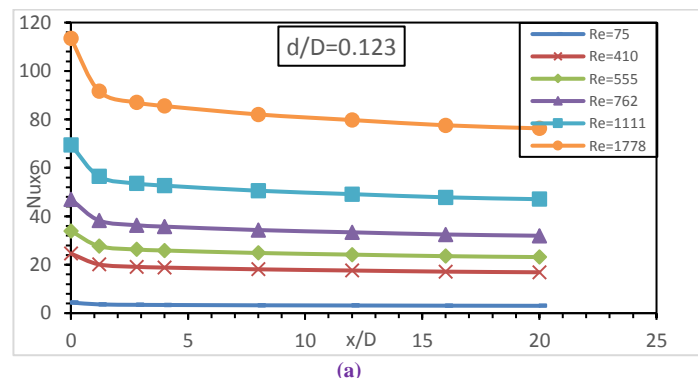


Fig. 6. Influence of Reynolds Number on the entrance length for different diameter ratios for sphere particles and PEO concentration.

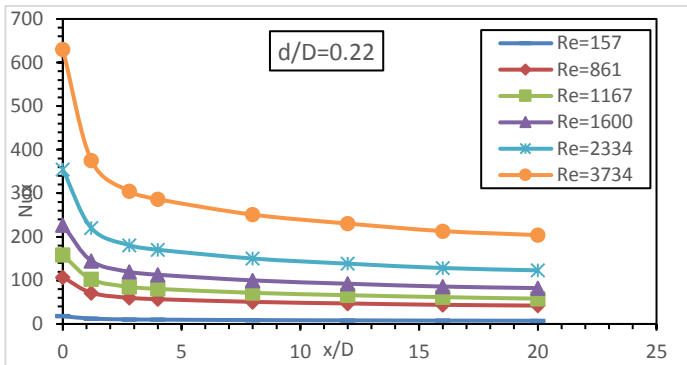
B. Local Nusselt number

Figure 7 illustrates the local Nusselt number variation for water flow along the length of the pipe for different values of Reynolds number at different diameters of plastic sphere particles. It shows that the local Nusselt number decreases with (x/D) along the length of the pipe and increases with the increase of Reynolds number.

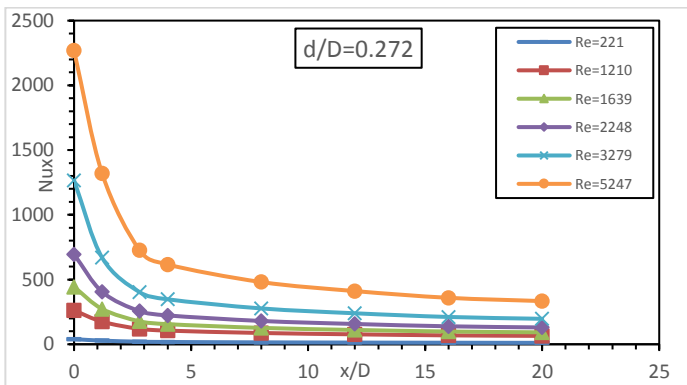
Figure 8 shows the relation between the local Nusselt number and (x/D) at various values of diameter ratios with a nearly constant Reynolds number, $Re \approx 1611$. The figure shows that the local Nusselt number increases with increasing diameter ratios, and the local Nusselt number depends on the diameter ratios.



(a)



(b)



(c)

Fig. 7. The local Nusselt number Variation with (x/D) for various values Reynolds number and different diameter ratios of plastic sphere particles for water flow.

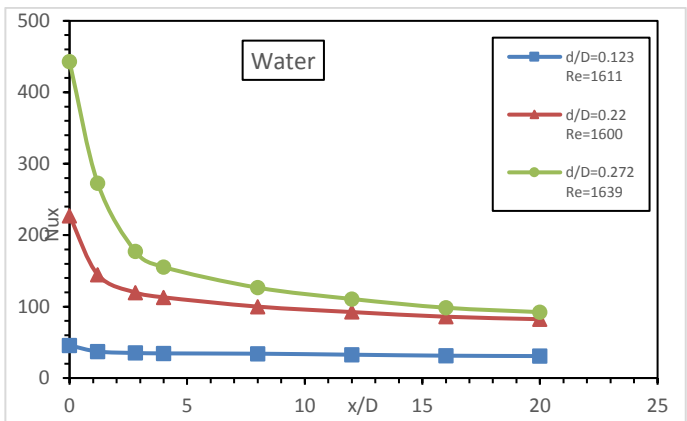


Fig. 8. Variation of the local Nusselt number with (x/D) at various values of diameter ratios at a nearly constant Reynolds number.

Figure 9 shows the relationship between local Nusselt number and tube length (x/d) for both water and different PEO concentrations at (50, 100, 150, and 200 ppm) while there are three different values of Reynolds number for each case of the diameter ratios $d/D = 0.123, 0.22,$ and $0.272,$ respectively. It is found that the local Nusselt number does not depend on the PEO concentration but only on Reynolds number and diameter ratio.

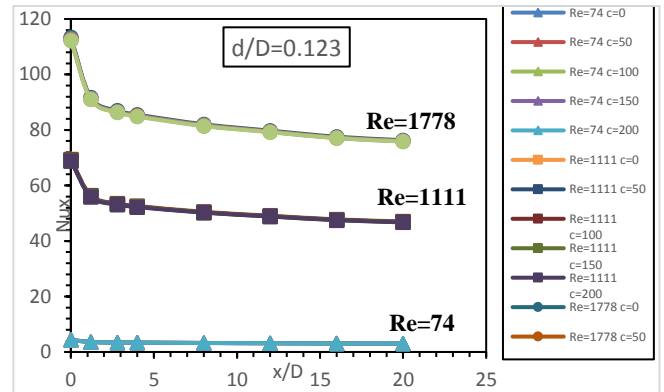


Fig. 9 (a) Variation the local Nusselt number with (x/D) at $d/D=0.123$ at three constant values of Reynolds number for water and different values of concentration at (50, 100,150, and 200) ppm.

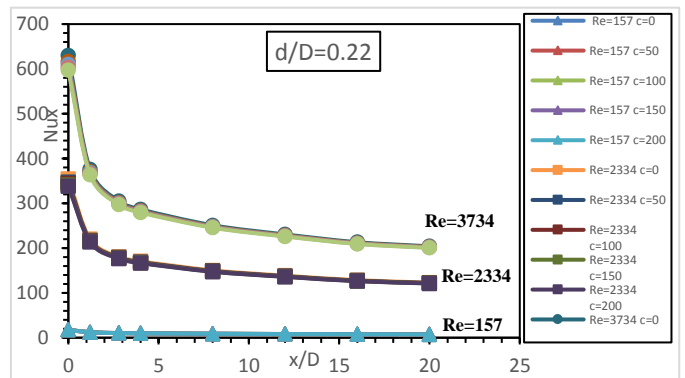


Fig. 9. (b) Variation the local Nusselt number with (x/D) at $d/D=0.22$ at three constant values of Reynolds number for water and different values of concentration at (50, 100,150, and 200) ppm.

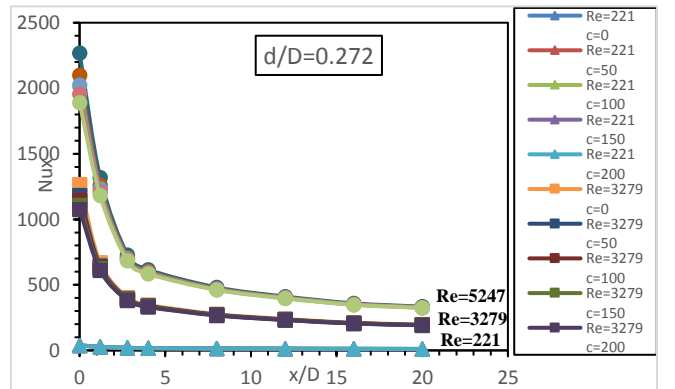


Fig. 9. (c) Variation the local Nusselt number with (x/D) at $d/D=0.272$ at three constant values of Reynolds number for water and different values of concentration at (50, 100,150, and 200) ppm.

C. Nusselt Number

Figures 10 and 11 demonstrate the relationship between Nusselt number and PEO concentration. Figure 10 demonstrates that if Reynolds number is constant for all concentrations, the average Nusselt number will not depend on the concentration. To obtain the same Reynolds number value at all concentrations, the speed has been carefully adjusted to give approximately the same Reynolds number at each concentration. Two values for Reynolds number are used: 157 and 2334 at all concentrations, and it is shown from the figure

that Nusselt number does not depend on changing the concentration but only on changing Reynolds number.

Figure 11 shows the relation between Nusselt number and PEO concentration flow with changing the diameter ratios $d/D = 0.123, 0.22, \text{ and } 0.272$, for constant Reynolds = 1778. It is found that Nusselt number is not affected by the change of PEO concentration, but it is affected by the change in the diameter ratios.

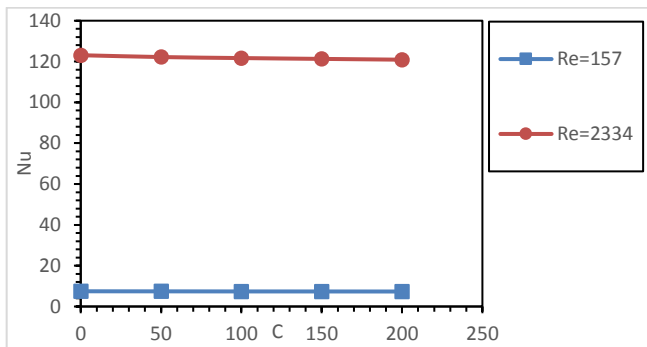


Fig. 10. The variation of Nusselt number with concentration at constant two values of Reynolds number.

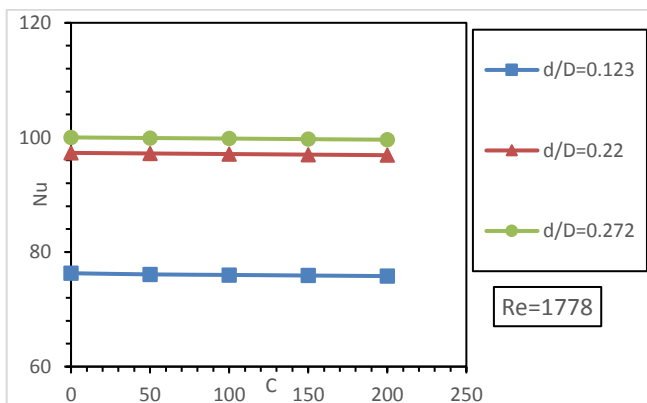


Fig. 11. The variation of Nusselt number with PEO concentration at various values of Diameter ratios (d/D).

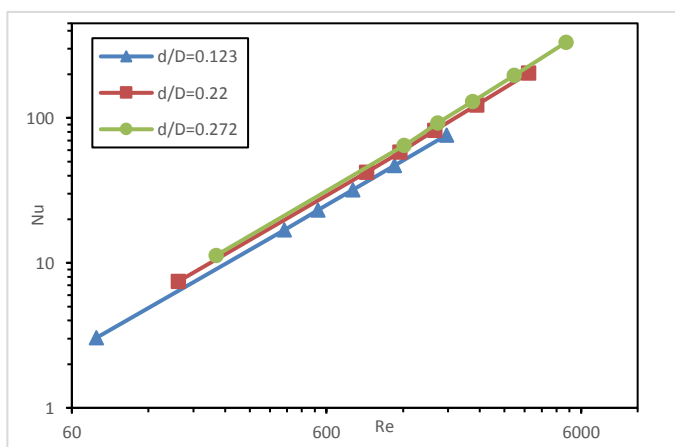


Fig. 12. Variation of Nusselt number with Reynolds number for different diameter ratios for plastic sphere particles.

Figure 12 presents Nusselt number with the variation of Reynolds number for water at different diameter ratios $d/D = (0.123, 0.22, \text{ and } 0.272)$. The figure shows that Nusselt number increases with increase of Reynolds number for water flow. Nusselt number increases as the diameter of the sphere of particles and porous media filled in a pipe increases. Nusselt number increases with the diameter ratio d/D . And Nusselt number depends only on Reynolds number and the diameter ratio (d/D).

Curve fitting for experimental results in the range of Reynolds number and polymer concentration shows Nusselt number is related to Reynolds number and diameter ratio d/D as follows:

$$Nu = 0.0355 Re^{1.065} (d/D)^{0.035} \quad (14)$$

for Reynolds number $74.93 \leq Re \leq 5247.3$ and diameter ratio $0.123 \leq d/D \leq 0.272$.

VI- CONCLUSION

An experiment is conducted to determine the effect of Reynolds number and PEO concentrations on Nusselt number and heat transfer coefficients for water and drag reducing fluid flow in a pipe filled with plastic spheres as porous media. Different diameter ratios (d/D) for sphere particle porous media (0.123, 0.22, and 0.272) and a different concentration of (50, 100, 150, and 200) ppm for polyethylene oxide polymer (drag reducing fluid) are used. The results show:

1) The thermal entrance length is independent on the PEO concentration and the diameter ratios but depends only on Reynolds number.

2) A correlation of the thermal entrance length with Reynolds number is obtained as follows:

$$Xe/D = 0.0284 Re^{0.5663}$$

3) The local Nusselt number for water and drag reducing (polyethylene oxide) flow decreases along with the length of the pipe.

4) The local Nusselt number and Nusselt number increase as the diameter ratio (d/D) of sphere particles increases.

5) The local Nusselt number and Nusselt number are independent on the PEO concentration.

6) Nusselt number depends only on Reynolds number and diameter ratios (d/D).

7) A correlation of the average Nusselt number with the variation of Reynolds number and the diameter ratio d/D is obtained as follows:

$$Nu = 0.0355 Re^{1.065} (d/D)^{0.035}$$

for Reynolds number $74.93 \leq Re \leq 5247.3$ and diameter ratio $0.123 \leq d/D \leq 0.272$.

Funding: The authors should mention if this research has received any type of funding.

Conflicts of Interest: The authors should explicitly declare if there is a conflict of interest.

NOMENCLATURE

Symbols

C	Polymer concentration	(-)
C_n	New required concentration	(-)
C_{st}	Stock concentration	(-)
C_p	Specific heat for water	(kJ/kg K)
d	Particle diameter	(m)
D	diameter of pipe	(m)
h	Heat transfer coefficient	(W/m ² K)
k_f	Thermal conductivity	(W/m K)
l	Test section length	(m)
m_s	Solute mass	(mg)
M_w	Molecular weight	(g/mole)
Nu	Nusselt Number	(-)
ppm	Particle per millions	(-)
q	wall heat flux per unit area	(W/m ²)
Q_w	wall heat flux	(W)
Re	Reynolds number	(-)
T	Temperature	(K)
T_m	Mean Temperature	(K)
T_w	Wall Temperature	(K)
X	Length of pipe	(m)
X_e	Thermal entrance length	(m)
V_{st}	Volume of the stock	(liter)
V_w	Water volume	(liter)

Greek symbols

ε	Porosity	(-)
μ	Viscosity	(kg/m.s)
ρ	Density	(kg/m ³)

REFERENCES

- Huang, T., Du, P., Peng, X., Wang, P., & Zou, G. (2020). Pressure drop and fractal non-Darcy coefficient model for fluid flow through porous media. *Journal of Petroleum Science and Engineering*, 184, 106579.
- Ghalambaz, M., Ayoubi Ayoubloo, K., & Hajjar, A. (2020). Melting heat transfer of a non-Newtonian phase change material in a cylindrical vertical-cavity partially filled porous media. *International Journal of Numerical Methods for Heat & Fluid Flow*, 30(7), 3765-3789.
- Gong, W., Shen, J., Dai, W., Li, K., & Gong, M. (2021). Research and applications of drag reduction in thermal equipment: A review. *International Journal of Heat and Mass Transfer*, 172, 121152.
- Ali, Q. M. A., & Al-ausi, T. A. (2008). Drag force reduction of flowing crude oil by polymers addition. *Iraqi journal of mechanical and material engineering*, 8(2), 149-161.
- Asidin, M. A., Suali, E., Jusnukin, T., & Lahin, F. A. (2019). Review on the applications and developments of drag reducing polymer in turbulent pipe flow. *Chinese Journal of Chemical Engineering*, 27(8), 1921-1932.
- Rabie, L. H., & Mostafa, H. (2001). Heat Transfer in Laminar Pulsating Annular Flow of Drag Reducing Dilute Polymer Solutions. (Dept. M). *MEJ. Mansoura Engineering Journal*, 26(2), 15-27.
- Raei, B., Shahraki, F., & Peyghambarzadeh, S. M. (2018). Experimental study of the effect of drag reducing agent on heat transfer and pressure drop characteristics. *Experimental Heat Transfer*, 31(1), 68-84.
- Lv, F. Y., & Zhang, P. (2016). Drag reduction and heat transfer characteristics of water flow through the tubes with superhydrophobic surfaces. *Energy Conversion and Management*, 113, 165-176.
- Sears, P. L., & Yang, L. (2006). Heat Transfer in a Surfactant Drag-Reducing Solution—A Comparison with Predictions for Laminar Flow.
- Varnaseri, M., & Peyghambarzadeh, S. M. (2020). The effect of polyacrylamide drag reducing agent on friction factor and heat transfer coefficient in laminar, transition and turbulent flow regimes in circular pipes with different diameters. *International Journal of Heat and Mass Transfer*, 154, 119815.
- Chamkha, A. (2010). Heat and mass transfer of a non-Newtonian fluid flow over a permeable wedge in porous media with variable wall temperature and concentration and heat source or sink.
- Rashad, A. M., Chamkha, A. J., & Abdou, M. M. M. (2013). Mixed convection flow of non-Newtonian fluid from vertical surface saturated in a porous medium filled with a nanofluid
- Tian, X. W., Xu, S. M., Sun, Z. H., Wang, P., Xu, L., & Zhang, Z. (2018). Experimental study on flow and heat transfer of power law fluid in structured packed porous media of particles. *Experimental Thermal and Fluid Science*, 90, 37-47.
- Kairi, R. R., & Murthy, P. V. S. N. (2011). Effect of viscous dissipation on natural convection heat and mass transfer from vertical cone in a non-Newtonian fluid saturated non-Darcy porous medium. *Applied Mathematics and Computation*, 217(20), 8100-8114.
- Peixinho, J., Desaubry, C., & Lebouche, M. (2008). Heat transfer of a non-Newtonian fluid (Carbopol aqueous solution) in transitional pipe flow. *International journal of heat and mass transfer*, 51(1-2), 198-209.
- Rao, B. K. (2002). Internal heat transfer to power-law fluid flows through porous media. *Experimental heat transfer*, 15(2), 73-87.
- Zhang, X., Liu, L., Cheng, L., Guo, Q., & Zhang, N. (2013). Experimental study on heat transfer and pressure drop characteristics of air–water two-phase flow with the effect of polyacrylamide additive in a horizontal circular tube. *International Journal of Heat and Mass Transfer*, 58(1-2), 427-440.
- Shenoy, A. V. (1994). Non-Newtonian fluid heat transfer in porous media. In *Advances in Heat transfer* (Vol. 24, pp. 101-190). Elsevier.
- El-Kady, M. S. Z. (1996). Forced Convection Heat Transfer In a Cylindrical Porous Media exposed to Constant Wall Heat Flux. (Dept. M). *MEJ. Mansoura Engineering Journal*, 20(2), 88-103.
- Ai-Hamad, M., & Duwairi, H. M. (2013). Effect of Heat Generation/Absorption on Heat Transfer for a Non-Newtonian Fluid. *International Journal of Heat and Technology*, 26, 115-120.
- Atwan, E. F., El-Shamy, A. R., & El-Shazly, K. M. (2000). An experimental study of forced convection in horizontal porous annuli. In *Al-Azhar Engineering Sixth International Conference*.
- El Kady, M. S., Araid, F. F., Abd El Aziz, G. B., El-Negiry, E. N., & Abd El-Latief, E. (1999). Effect of Porosity on The Natural Convection Heat transfer in an Inclined Annular Porous Medium. (Dept. M). *MEJ. Mansoura Engineering Journal*, 24(2), 1-11.
- El-Kady, M. S. (2002). Effect of Operating Conditions on the Mixed Convection in a Channel with Discrete Heat Sources and Partially Filled with Porous Media. (Dept. M). *MEJ. Mansoura Engineering Journal*, 27(4), 47-61.
- Mahgoub, S. E. (2013). Forced convection heat transfer over a flat plate in a porous medium. *Ain Shams Engineering Journal*, 4(4), 605-613.
- Zhang, M., Zhao, Q., Huang, Z., Chen, L., & Jin, H. (2021). Numerical simulation of the drag and heat-transfer characteristics around and through a porous particle based on the lattice Boltzmann method. *Particuoogy*, 58, 99-107.
- Abdul Latif, K., Marghany, E., Ragab, M., Mansour, M. H., Rabie, L. H., & El Kady, M. S. (2022). Non-Newtonian Drag Reducing Flow Characteristics in Porous Media. *Journal of Engineering Research*, 6(5), 1-6.
- Alam, M. A., & Vikas, A. C. (2017). Drag reduction of flow through packed bed material using natural polymer, *International Journal of Engineering Science & Research Technology*